



Science Arts & Métiers (SAM)

is an open access repository that collects the work of Arts et Métiers ParisTech researchers and makes it freely available over the web where possible.

This is an author-deposited version published in: <https://sam.ensam.eu>
Handle ID: <http://hdl.handle.net/10985/17135>

To cite this version :

Sajid BUTT, Jean-François ANTOINE, Patrick MARTIN - Simplified stiffness model for spherical rough contacts - Tribology - Materials, Surfaces & Interfaces - Vol. 9, n°2, p.63-70 - 2015

Any correspondence concerning this service should be sent to the repository

Administrator : archiveouverte@ensam.eu



Simplified stiffness model for spherical rough contacts

S. U. Butt*¹, J.-F. Antoine² and P. Martin²

Obtaining a surface with negligible roughness is very expensive, time consuming and unnecessary. The influence of surface roughness on the contact stiffness is of great importance. The extra cost associated with unnecessary surface finish can be limited by eliminating the unnecessary machining operations beyond the required surface finish. In this article, a simplified solution is presented to calculate the stiffness of rough contact between the workpiece and spherical locator; also, the effect of surface roughness on the stiffness and deformation of rough spherical contact is studied for different applied loads to find an 'economic roughness' under machining forces.

Keywords: Analytical model, Contact mechanics, Rough contact, Contact stiffness, Contact deformation

List of symbols

a_H maximum radius of Hertzian contact area, m
 a_L maximum radius of rough contact area, m
 a'_L non-dimensional radius of macrocontact, $a'_L = a_L/a_H$
 H_{mic} microhardness
 M second non-dimensional parameter
 P radius of curvature, m
 P_0 maximum pressure distribution, $N m^{-2}$

$P_{0,H}$ maximum Hertzian pressure distribution, $N m^{-2}$
 P'_0 non-dimensional maximum pressure distribution
 T first non-dimensional parameter
 α roughness parameter, $\alpha = \sigma\rho/a_H^2$
 δ_C deformation of rough contact, m
 $\delta_C(0)$ deformation at centre of rough contact, m
 δ_H ideal Hertz deformation, m
 σ rms surface roughness R_T , m
 ξ non-dimensional radial position of contact, $\xi = r/a_L$

Introduction

Hertzian contact theory was established to predict the behaviour of ideally smooth contacting surfaces assuming their contacts to be purely elastic. However, real engineering surfaces are rough at microscopic level, and their interactions involve the contact of surface peaks at discrete spots called asperity tips.¹ This surface roughness affects the contact behaviour, and real contact area becomes smaller than the one calculated by Hertzian contact theory. Hertz replaced contacting spherical surfaces with paraboloids, so that the contact between two spheres is simplified to sphere–plane contact with the sphere having equivalent radius given by $1/\rho = 1/\rho_1 + 1/\rho_2$. For the calculation, the sphere is assumed to be rigid, and only the half space supports deformation. An effective modulus of elasticity is defined for this half space, which is $1/E' = (1 - \nu_1^2)/E_1 + (1 - \nu_2^2)/E_2$. Hertz pressure distribution on the contact is written in equation (1)²

$$P_H(r/a_H) = P_{0,H} [1 - (r/a_H^2)]^{1/2} \quad (1)$$

Analytical models defining $A = 1/\rho_1$ and $B = 1/\rho_2$ as principal curvature radii can be found in Refs. 3–5 to calculate the contact area for the elastic Hertzian elliptical contacts. Greenwood⁶ performed a comparison of all the three models^{3–5} for principle curvature range of $1 \leq B/A \leq 25$. The approach of Houpert⁷ provides maximum Hertzian pressure and Hertzian deformation as a function of the dimensionless load parameter for $B/A \leq 13,576$. Antoine *et al.*⁸ proposed an analytical formulation dedicated to rolling bearings and whose single formula fits the Hertzian theoretical values for a large range of B/A ratio with the precision of 0.006%.

For rough contact calculations, the problem of asperities can be encountered similar to the contact of two spheres. The contact of two rough surfaces is dealt as the contact between an ideally smooth surface and a rough surface having an equivalent surface roughness $\sigma = [\sigma_1^2 + \sigma_2^2]^{1/2}$.² A fast Fourier transform based deterministic model of elastic contact between rough surfaces is presented in⁹. The model predicted contact areas and forces from various elastic contact models using different roughnesses of the contacting surfaces. Malayalamurthi and Marappan¹⁰ used finite element analysis approach to model the contact area and contact pressure of an elastic–plastic contact between a sphere and a rigid flat surface. It was concluded that the material having $E/Y < 300$ exhibit different behaviours, while for $300 < E/Y < 1000$, the contact is fully plastic.

¹Department of Mechanical Engineering, College of Electrical and Mechanical Engineering, National University of Sciences and Technology (NUST) Islamabad, Pakistan

²LCFC, Arts et Métiers ParisTech, Metz 57078, France

* Corresponding author, email sajidullahbutt@ceme.nust.edu.pk

Other elastic–plastic contact models based on finite element analysis of a single asperity are proposed in Refs. 11 and 12. The models predicted contact parameters as the functions of plasticity index and contact load. Static friction coefficient was highly dependent upon the surface roughness through plasticity index.

Jackson and Green¹³ also used finite element method to model an elastic–perfectly plastic sphere in frictionless contact with a rigid flat surface. Their work accounts the contact geometry and material effects on overall behaviour of the contact. The contact area, force and pressure were found to be dependent upon the deformed geometry in all regimes and effectively dependent upon the material properties (e.g. strength) in the elastoplastic and plastic regimes.

Beheshti and Khonsari¹ compared the effect of surface roughness on contact characteristics, like contact pressure distribution, maximum contact pressure, contact width and the real contact area, through existing contact models of Kogut and Etsion,^{11,12} Jackson and Green,¹³ Greenwood and Williamson,¹⁴ Zhao and Maietta¹⁵ and Chang *et al.*¹⁶

The first analytical study for the effect of roughness on spherical contact was performed by Greenwood and Tripp.¹⁷ Their work was based on the elastic deformation, and it presented the deformation produced by an arbitrary pressure over the circular half space. The model was based on two non-dimensional parameters: T and μ . It was shown that the contact area was directly while the pressure was inversely proportional to the contact roughness. This model is complex and requires extensive numerical calculations. Furthermore, the parameters β and η cannot be measured directly and are estimated through statistical calculations. Additionally, these parameters are sensitive to surface measurements.^{2,18}

Mikic and Roc¹⁹ proposed an alternate numerical solution considering plastic deformation of asperities, but they did not report a generalised relation to calculate the contact parameters. Greenwood *et al.*²⁰ generalised the results of both previous models^{17,19} in terms of a single non-dimensional roughness parameter α , which is a function of surface roughness and radius of curvature ($\alpha = \sigma\rho/a_H^2$). It was concluded that the contact pressure is governed by α , and if the value of α is <0.05 , the effect of roughness becomes negligible and Hertzian theory may be applied.

Jourani²¹ proposed an elastoplastic model using the concept of representative strain to calculate the effect of surface roughness on real contact area and pressure distribution on flat contacting surfaces. He calculated the asperity deformation as the function of applied load and pressure and concluded that the real contact area remains a small fraction of apparent contact area. This model has been compared with the spherical approach and the spectral method using unidirectional ground and sanded surfaces. It was concluded that, for a surface with a low roughness, the elastic approach is sufficient to model the rough contact. However, for surfaces having a great roughness, the elastoplastic approach is more appropriate to determine the real area of contact and pressure distribution.

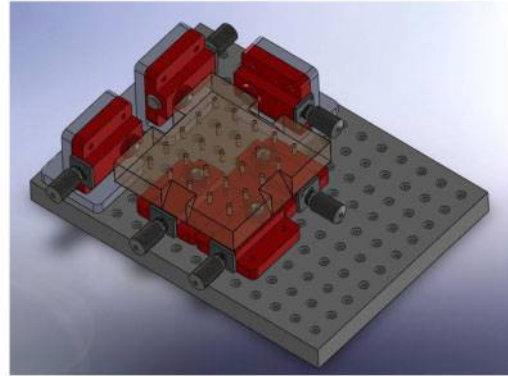
Bahrami *et al.*²² concluded that the maximum pressure distribution is the key parameter in rough contact calculations. A generalised pressure distribution is

proposed, which is valid for whole range of rough contacts. An analytical model was proposed, which was valid for all the experimental results of all the previous models^{17,19,20} for spherical rough contacts. The model of Bahrami *et al.*²² gives a close approximation to the experimental data, so their model is further simplified in this study without performing experiments.

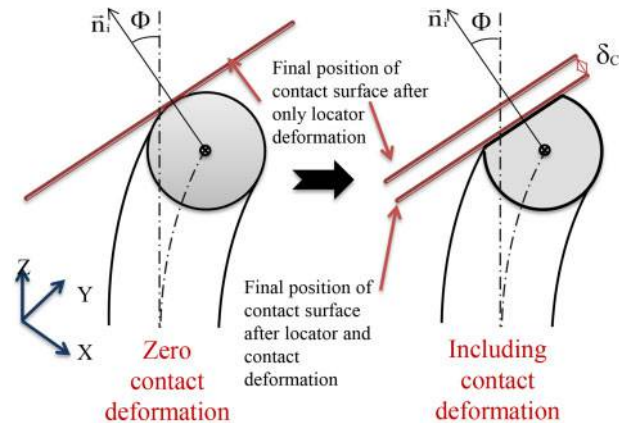
The work of Butt *et al.*²³ is divided in two parts: a kinematic model which helps to compensate the positioning error of the workpiece on machining fixture by the axial advancements of six supporting locators, and an analytical mechanical model which calculates the positioning error of the workpiece due to the deformation of elastic elements of the fixture. While the workpiece is under load, there will also be deformation at the contact of each of six locators (Fig. 1). Butt *et al.*²³ did not take the contact deformation into account for the final workpiece position calculation. They calculated total stiffness of the system by considering locator–baseplate contacts to be ideally smooth. Hertz contact theory was applied to the contacts, but in reality, the contact deformation depends upon the surface roughness and radius of curvature ($\alpha = \sigma\rho/a_H^2$).

The interest of this article is to find an explicit equation for maximum deformation of locator–workpiece contact at the centre of rough contact, which is proposed in the Bahrami model to be numerical. This helps the authors to calculate the total deformation of all

(a) Locators placement plant



(b) Effect of contact deformation on final position



1 Effect of locator deformation on final position of workpiece

the locators and, as a result, overall displacement of the workpiece on the supporting locators.²³ The solution also helps to limit the minimum and maximum roughness of contacting surfaces to keep the contact stiffness and deformation within acceptable limit. This proposed analytical solution is an extension of the solution obtained in Ref. 22 and a step forward to the solution proposed in Ref. 23. This article is composed as follows: the section on ‘Model of Bahrami’ briefly explains the solution of the spherical rough contacts as proposed in Ref. 22; the section on ‘Proposed model’ offers a simplified approximation for the beta function specific for the case of rough workpiece–locator contact (Fig. 1); in the section on ‘Application of the proposed model’, the effect of roughness on the global stiffness and deformation of rough contact is studied; and an application is illustrated in the last section to demonstrate the utility of the proposed model. This study justifies that the machining cost of unnecessary finish can be reduced by limiting the surface finish to a minimum value, which limits the contact deformation and stiffness to an acceptable value.

Model of Bahrami

Bahrami *et al.*²² showed that the non-dimensional maximum pressure distribution is the dominant parameter having maximum effect on the properties of rough contacts. Their model is based on the following hypotheses:

- (i) deformation mode of asperities is plastic
- (ii) bulk deformation of the contact is elastic, and all the bulk deformations occur at elastic half space with effective modulus of elasticity E'
- (iii) pressure at microcontacts is the microhardness of the softer contacting material
- (iv) surface roughness acts like plastic layer in the sense that the pressure distribution can be considered as continuous $P(r)$
- (v) the external pressure $P(r)$ is the sum of pressures at all microcontacts
- (vi) effective microhardness is constant throughout the contact area.

The non-dimensional pressure distribution for rough contacts γ and maximum pressure at the contact are presented in equations (2)–(4). These equations give Hertzian pressure distribution when contact roughness approaches to zero

$$P(\xi) = P_0(1 - \xi^2)\gamma \quad (2)$$

$$\gamma = 1.5 \frac{P_0}{P_{0,H}} \left(\frac{a_L}{a_H} \right)^2 - 1 \quad (3)$$

$$P_0 = (1 + \gamma) \frac{F}{\pi a_L^2} \quad (4)$$

The model²² is generalised in terms of two non-dimensional parameters: the first parameter is α ,²⁰ while the second is $\tau = (E'/H_{mic})\sqrt{\rho/\sigma}$. The equations for non-dimensional pressure (equation (5)) and non-dimensional contact area (equation (6)) are obtained by

curve fitting

$$P'_0 = \frac{1}{1 + 1.22\alpha\tau^{-0.16}} \quad (5)$$

$$a'_L = \begin{cases} 1.605/(P'_0)^{1/2} & 0.01 \leq P'_0 \leq 0.47 \\ 3.51 - 2.51P'_0 & 0.47 \leq P'_0 \leq 1 \end{cases} \quad (6)$$

Maximum deviation of equations (5) and (6) from the real models^{20,24,25} is claimed to be <4.5%. As calculation of a'_L involves testing for each value of pressure P'_0 , Bahrami²⁶ proposed a single equation (7) to approximate a'_L .

$$a'_L = \frac{a_L}{a_H} = 1.80 \frac{(\alpha + 0.31\tau^{0.056})^{1/2}}{\tau^{0.028}} \quad (7)$$

The numerical results of Bahrami model (equation (6)) are valid over full range of rough contacts. In the problem under consideration (Fig. 1), the maximum deformation occurs at the centre of the contact, i.e. $\xi = r/a_L=0$. This deformation is shown in equation (8) as proposed in Ref. 22

$$\delta_c(0) = \frac{P_0 a_L}{E'} B(0.5, \gamma + 1) \quad (8)$$

where B is beta function giving the maximum deformation value numerically. Bahrami *et al.*²² proposed an analytical solution of the deformation at the border of rough contact ($\xi = 1$), but no analytical solution was formulated for calculation of maximum deformation at the centre of rough contact. In this article, an analytical approximate solution of the non-dimensional contact area is proposed to obtain the contact deformation and stiffness of a rough sphere–plane contact (Fig. 1) using the previously explained parameters a'_L and P'_0 .

Proposed model

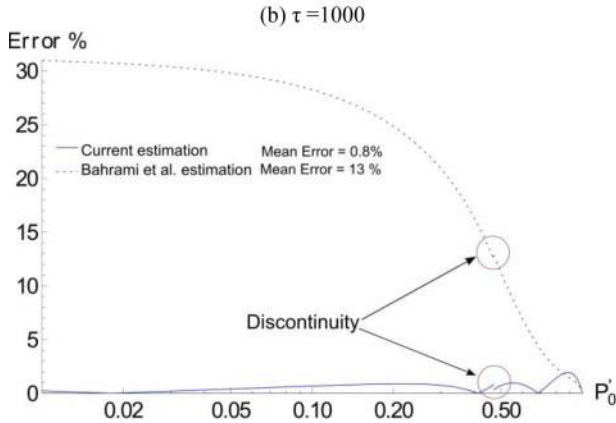
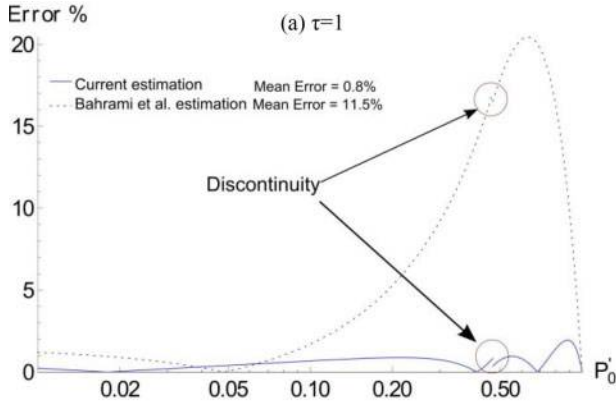
Here, a single analytical equation for non-dimensional contact area is proposed to avoid the testing of P'_0 in the Bahrami model. Later, a beta function approximation is performed for small values of γ in equation (8).

Non-dimensional contact area estimation

The curve fitted non-dimensional contact area (equation (6)) is compared with the estimated contact area of the Bahrami model (equation (7)), and the error is evaluated for different values of α and τ . An error of up to 30% has been revealed for some values of τ and α as shown in Fig. 2. This highlights the need of an explicit equation having more precise estimated value of contact area. For this purpose, a more precise equation is proposed for the estimation of a'_L for all values of P'_0 , which is further a function of τ and α . Estimation is performed by plotting equation (6) for all values of a'_L , and then by fitting the power equation curves with minimum least square error. New proposed function of non-dimensional contact area is presented in equation (9)

$$a'_{L,new} = 1.631 P_0^{-0.496} - 0.631 P_0^{3.358} \quad (9)$$

where P'_0 can be evaluated through equation (5). Proportional coefficients 1.631 and 0.631 are chosen to keep the border condition ($a'_L(P'_0 = 1) = 1$) valid. This proposed estimated contact area (equation (9)) is compared with the estimated contact area²⁶ (equation (7)) for two



2 Comparison of proposed and Bahrami error for a'_L

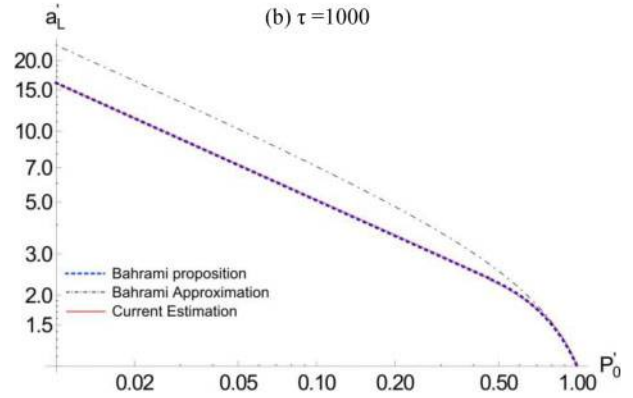
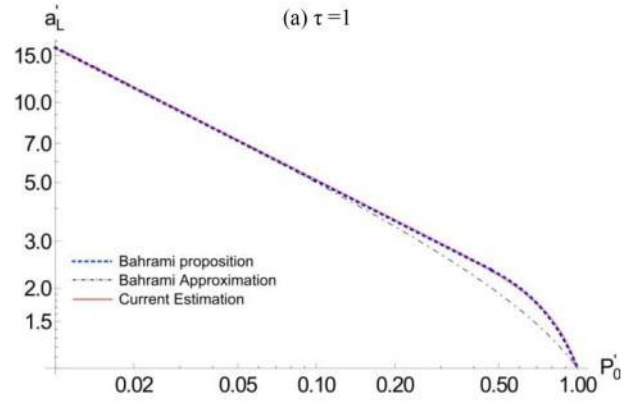
different values of τ (1 and 1000) in Fig. 3, and their relative error is compared in Fig. 2. Curves in Fig. 2 are discontinuous; it is only because the actual function of Eq. (6) is discontinuous at $P'_0 = 0.47$.

The model of Bahrami is claimed to give a close approximation to the experimental data; therefore, by taking equation (6) to be a valid formulation, it can be seen in Fig. 2 that equation (9) describes the non-dimensional contact area with least error for all values of α and τ , and it is convenient to replace equation (6) with the proposed equation (9).

The next step is to estimate the deformation at the centre of contact calculated in terms of beta function, which is calculated in terms of beta function in Ref. 22 and is shown in equation (8).

Beta function estimation

In the problem under consideration (Fig. 1), the deformation at the centre of contacting surfaces for all the locators is to be calculated for the precise position of the workpiece in machine's frame of reference. An algorithm helps the position of the workpiece to converge to the final position iteratively. The iterative calculations slow down due to these numerical functions. An explicit approximation of beta functions is necessary to obtain quick results. For this purpose, an approximation is proposed, which satisfies the results from the numerical solution of equation (8) with minimum error. By investigating the numerical result, it is observed that the beta function is further a function of 'gamma function (Γ)' (equation (10)), again a numerical value



3 Comparison of proposed and Bahrami estimation for a'_L

$$B(x, y) = \frac{\Gamma(x)\Gamma(y)}{\Gamma(x+y)} \quad (10)$$

Gamma function

In ^{27,28}, the complete gamma function $\Gamma(z)$ is defined by the improper integral $\int_0^\infty e^{-t} t^{z-1} dt$ for $z > 0$. It is also defined to be an extension of factorial to complex and real number arguments presented by L. Euler (in 1729). It is related to the factorial by the relation $\Gamma(z) = (z-1)!: z \in N$, where N is positive integer.

Estimation models like Stirling approximation²⁸ and Gergö approximation²⁹ for gamma functions are available in the literature. Gergö approximation is similar to Stirling approximation but easier to use. The problem under consideration (Fig. 1) involves very small values of γ (equation (3)), while Gergö and Stirling approximations are the approximations of large factorials, and they produce large errors for very small values of γ . An analytical estimation needs to be formalised, which describes the beta function for small values of γ as well for this specific case of rough contacts. For this purpose, an analytical expression for gamma function estimation is obtained by least square parameter optimisation over a large range of γ values. This analytical equation is presented in Eq. (11). Beta function can further be obtained using equation (10)

$$\Gamma(b+1) = a_1(b+a_2)^{b+a_2} \times \left(1 + \frac{a_3}{a_4 + b^{a_5}} + \frac{a_6}{b^{a_7} + a_8}\right) e^{-b^{a_9}} (2\pi)^{1/2} \quad (11)$$

where a_1, \dots, a_9 are the parameters, and their optimal values are shown in Table 1. A comparison of errors in gamma and beta function using equation (11) is presented in Fig. 4, where absolute values of errors in beta and gamma functions are plotted in logarithmic scale. Higher values of parameter γ cause the cumulative error to often return the infinity as seen in Fig. 4a.

The proposed expression for gamma function gives better results for small values of γ , which is of great interest for the problem under consideration (Fig. 1). Other asymptotic models are more efficient for large values of γ , but their calculation produces noise for very large values of γ . The proposed model shows a homogeneous absolute error for all values of γ . Hence, it can be concluded that the proposed model gives better accuracy for the surfaces having small γ values.

The deformation at the centre of rough contact can be calculated as a function of σ from equations (8)–(11) without testing of P_0 (equation (6)).

Contact stiffness

Overall stiffness of the system depends upon the stiffness of each locator and their contact with the workpiece, but the contact stiffness depends upon the quality of the contacting surface. Estimating influence of surface roughness on the global contact stiffness is primordial for precise mechanical behaviour modelling. The relation between the force acting on a sphere–plane contact and its deformation δ_c at the centre is non-linear as shown in equation (12)³⁰

$$F = \kappa \delta_c(0)^{3/2} \quad (12)$$

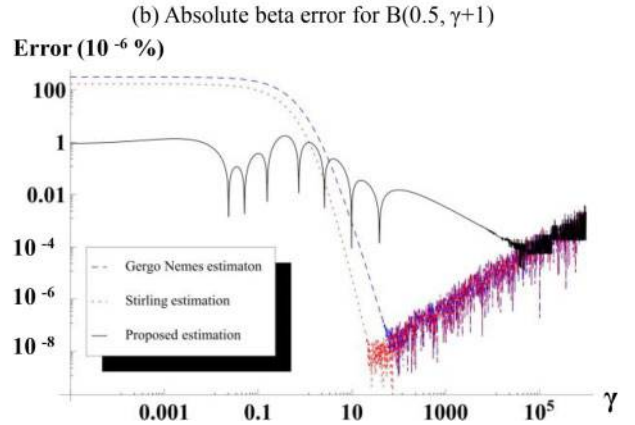
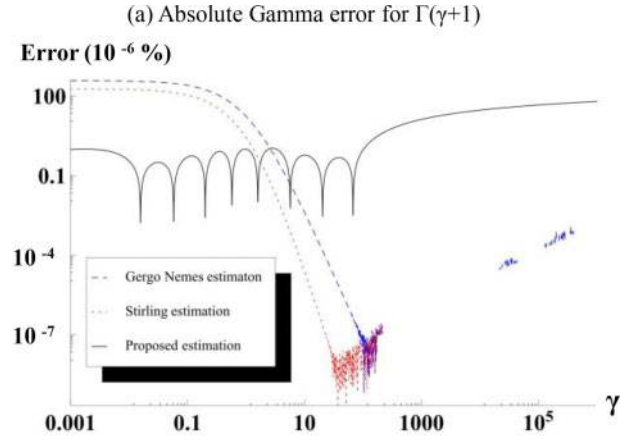
where $\kappa = (16RE^2/9)^{1/2}$. Differential of equation (12), with respect to displacement, furnishes the stiffness on the contact, which is

$$\kappa_c = \frac{3}{2} \kappa [\delta_c(0)]^{1/2} \quad (13)$$

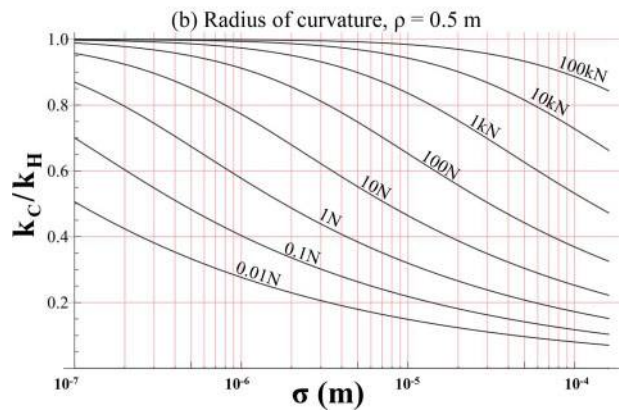
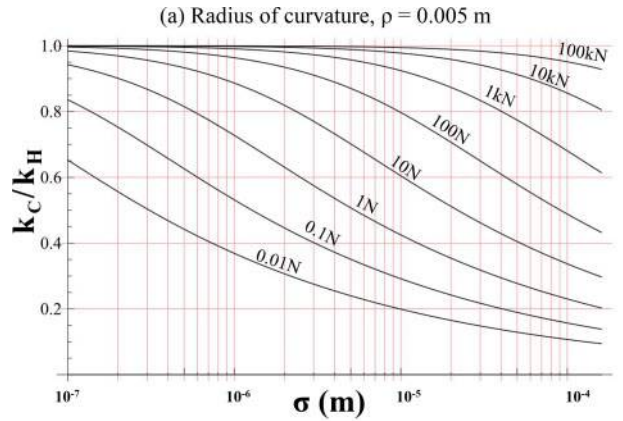
Contact stiffness is the function of applied force, material of locator and workpiece and α . The non-dimensional parameter α is further a function of surface roughness and radius of curvature ($\alpha = \sigma\rho/a_H^2$). For the problem under consideration (Fig. 1), the σ affects more on the contact stiffness as compared to ρ . Hertz stiffness K_H is calculated for ideal smooth surface. The ratio of theoretical stiffness of rough surface and ideal Hertz stiffness (K_c/K_H) is plotted against surface roughness (σ) for two different values ρ (0.5 and 0.005 m) in Fig. 5. The forces acting on the contact is changed from 0.01 N to 100 kN in Fig. 5. For realistic values, the stiffness ratio is plotted for the surface roughness range of $0.4\mu\text{m} \leq \sigma \leq 150\mu\text{m}$ for each value of force 10^j , where $j = -2, -1, \dots, 5$. It can be seen that, as the contact load increases and more asperities come in contact, the contact stiffness increases sharply.¹¹

Table 1 Optimised parameters in gamma function approximation

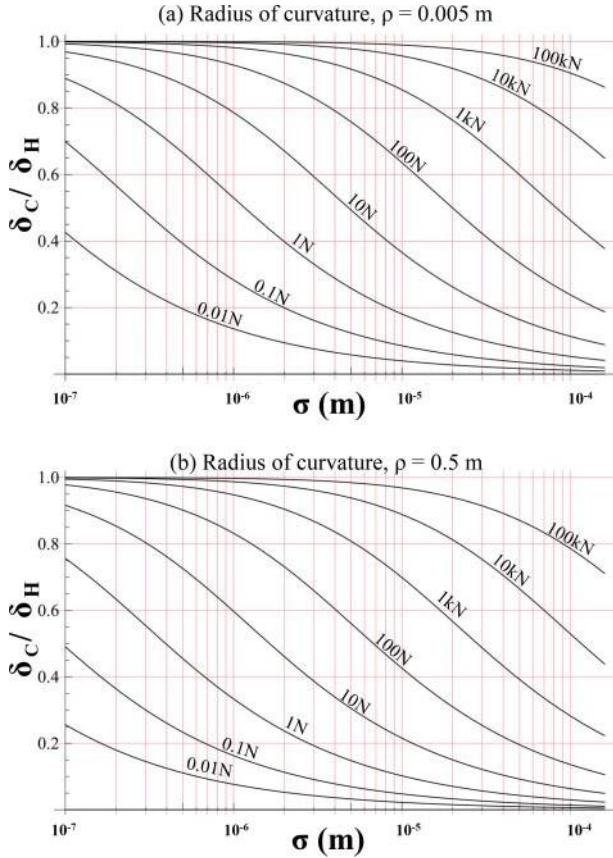
Par.	Value	Par.	Value
a_1	0.5641886354	a_2	0.500007096
a_3	0.1091637999	a_4	1.621840565
a_5	0.992925298	a_6	0.0115834573
a_7	1.271839956	a_8	1.505508639
a_9	1		



4 Comparison of proposed and existing approximations



5 Effect of contact's roughness on its relative stiffness for different applied loads



6 Effect of contact's roughness on its relative deformation for different applied loads

The real to Hertzian contact deformation is written as the function of stiffness ratio in equation (14). The effect of the roughness of contacting surface on the actual deformation as compared to the Hertzian ideal deformation for two different values ρ (0.5 and 0.005 m) is shown in Fig. 6

$$\frac{\delta_c}{\delta_H} = \left(\frac{K_C}{K_H} \right)^2 \quad (14)$$

Figs. 5 and 6 show that σ has more effect on the contact stiffness and deformation as compared to ρ . For less force, the surface roughness affects more on the stiffness

and the deformation of the rough contact for lesser forces. For high values of the normal forces, the effect of the roughness is negligible as compared to overall deformation of the contacting surfaces. For the same surface roughness, relative contact stiffness and deformation are directly related to applied load.

Similarly, the locators with less radius of curvature experience more deformation, so it is recommended to use the locators having large radius of curvature to reduce the contact deformation. The quality of the contacting surface has to be chosen according to the operating conditions as the contact deformation causes the geometrical deviation of the workpiece. After a value, unnecessarily extra finished surface will not have any necessary influence on the geometrical deviation. If the stiffness, that the part should exhibit to allow acceptable deformation under machining forces, is known, then an 'economic roughness' can be defined in order to avoid machining of unnecessary superfine surface. A complete set of equations, to calculate the deformation of the rough surfaces using the proposed model, is shown in Table 2.

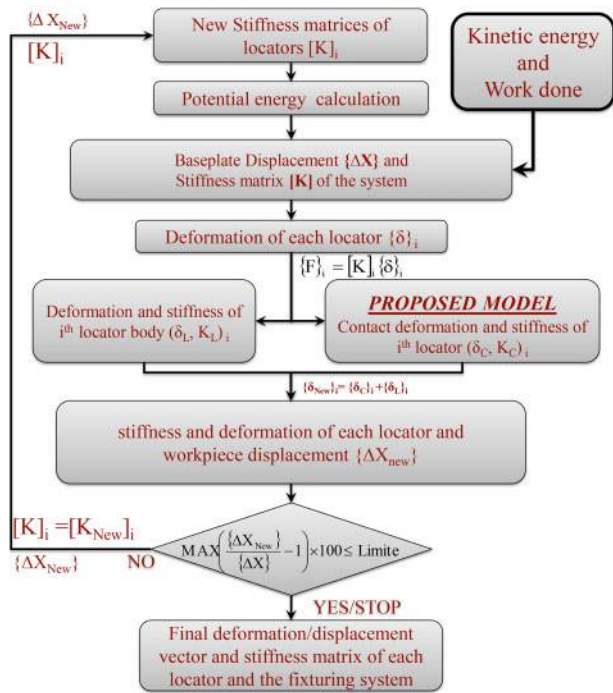
Application of proposed model

For the application of the proposed model, the case study is taken from Ref. 23. All the input data including the orientation of the baseplate, positions and points of contacts of the locators, magnitude and point of action of clamps and machining force are taken as in Ref. 23. The locators and baseplate are chosen to be made of steels having the elastic modulus to be 200 GPa and H_{mic} to be 20 GPa. As explained in Butt *et al.*,²³ stiffness of the fixture and displacement of the baseplate can be calculated with or without considering the effect of the contact. The flowchart to calculate the workpiece (baseplate) displacement is shown in Fig. 7³¹

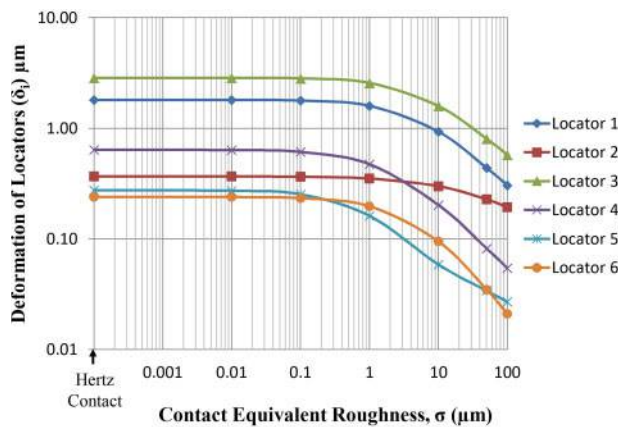
In this work, the main concern is to find the effect of contact roughness on deformation of each locator and overall displacement of the baseplate. Hertz contact theory is used to calculate the contact deformation and stiffness of all locators (Fig. 7) for ideally smooth contacts. The deformation of each locator and the displacement of baseplate, for ideally smooth contacts, are shown by left most points in Figs. 8 and 9 respectively.

Table 2 Equation set for calculating deformation of rough contact

Calculation steps	Equation
Hertz contact area	$a_H = \left(\frac{3F_p}{4E^*} \right)^{1/3}$
Roughness parameter	$\alpha = \sigma \rho / a_H^2$
First non-dimensional parameter	$\tau = \frac{E^*}{H_{mic}} \left(\frac{\rho}{\sigma} \right)^{1/2}$
Non-dimensional pressure distribution	$P'_0 = \frac{1}{1+1.22 \alpha \tau^{-0.16}}$
Non-dimensional contact radius	$a'_L = 1.631 P'_0^{-0.496} - 0.631 P'_0^{3.358}$
Generalised pressure distribution exponent	$\gamma = 1.5 P'_0 a'_L{}^2 - 1$
Area of rough contact	$a_L = a'_L a_H$
Max. contact pressure	$P_0 = (1 + \gamma) F / \pi a_L^2$
Estimated gamma function	$\Gamma(b+1) = a_1(b+a_2)^{b+a_2} \left(1 + \frac{a_3}{a_4+b^{a_5}} + \frac{a_6}{b^{a_7+a_8}} \right) e^{-b^{a_9}} (2\pi)^{1/2}$
Estimation of beta function	$B(0.5, \gamma+1) = \frac{\Gamma(1/2)\Gamma(\gamma+1)}{\Gamma(\gamma+1.5)}$
Contact deformation at $r = 0$	$\delta_c = \frac{P_0 a_L}{E^*} B(0.5, \gamma+1)$



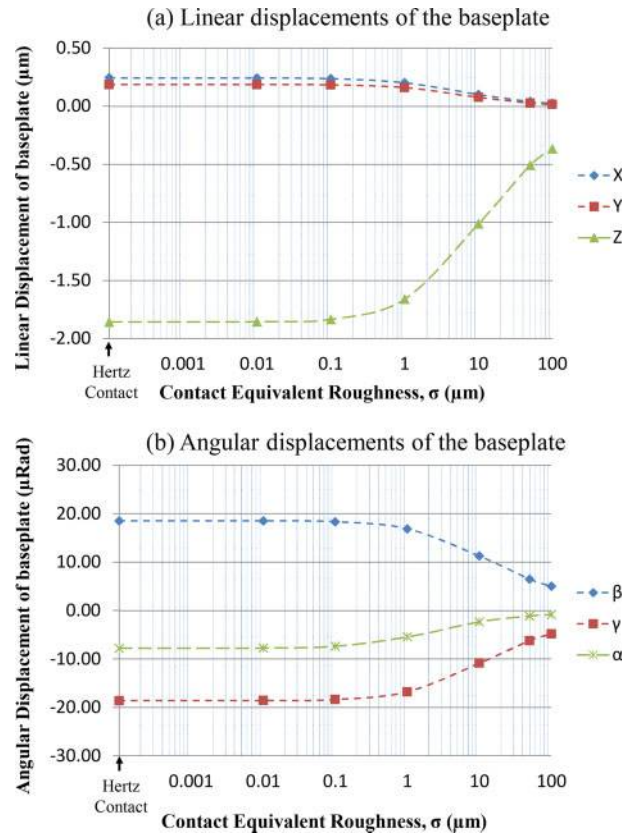
7 Flow chart of algorithm to calculate overall displacement³¹



8 Deformation of locators as function of equivalent contact roughness

To calculate the deformation of locators having rough contact and their effect on the baseplate displacement, the Hertz theory is replaced by the proposed model (Table 2). Force on each contact F_i can be calculated through the magnitude vector of force acting on each locator, while ρ , E' and H_{mic} are also known. In order to calculate the effect of surface roughness, σ is varied from 0.01 to 100 μm . As all the variables are known, the equations in Table 2 can be applied to calculate the deformation of each contact, and equation (13) can be used to calculate the contact stiffness to each locator. The deformation of each locator and the displacement of baseplate are shown in Fig. 8 and Fig. 9 respectively.

It can be seen from Figs. 8 and 9 that contact roughness is an important parameter in calculating the deformation of each locator and hence the final position of the workpiece (baseplate). For this specific case, the roughness affects the positioning error after it exceeds 0.5 μm and below that the effect of contact roughness is



9 Six degrees of freedom displacement of workpiece as function of equivalent contact roughness (a linear displacement; b angular displacement)

almost negligible. It can be concluded that extra finished contact surface is not needed to attain ideal results. For example, if the locators and baseplate having equivalent roughness of $<0.1 \mu\text{m}$ are used, the locators' deformations have a maximum deviation of 5% from the Hertz contact theory. The value of 'economic roughness' can be obtained depending upon the maximum allowable displacement of the workpiece. This limit can be changed by changing the system parameters.

Conclusions

A simplified analytical solution has been presented to calculate the stiffness of rough contact between a rectangular workpiece and spherical locator (Fig. 1) without any numerical resolution. A review of present models, describing the deformation of rough plane-sphere contact, has been presented. A simplified analytical solution has been proposed to calculate the contact area of rough plane-sphere contact. A generalised solution of deformation at the centre of contact has been replaced by a more simplified explicit solution in order to get quick result without the need of specialised mathematical tools. At the end, stiffness of the rough contact has been calculated and compared with the Hertzian contact stiffness. This comparison enables us to eliminate the cost related to extra finishing operation (beyond the need) and to fabricate the cost effective parts. An economic roughness can be defined to limit the contact deformation to the maximum allowed value.

Acknowledgements

The authors gratefully acknowledge the financial support from Higher Education Commission (HEC), Pakistan.

References

1. A. Beheshti and M. M. Khonsari: 'Asperity micro-contact models as applied to the deformation of rough line contact', *Tribol. Int.*, 2012, **52**, 61–74.
2. K. L. Johnson: 'Contact mechanics'; 1987, Cambridge, Cambridge University Press.
3. J. A. Greenwood: 'Formulas for moderately elliptical Hertzian contacts', *J. Tribol.*, 1985, **107**, 501.
4. D. E. Brewe and B. J. Hamrock: 'Simplified solution for elliptical-contact deformation between two elastic solids', *ASME, Trans. F*, 1977, **99F**, 485–487.
5. B. Hamrock and D. Brewe: 'Simplified solution for stresses and deformations', in 'Proc. American Society of Mechanical Engineers and American Society of Lubrication Engineers, Joint Lubrication Conf., New Orleans, LA, USA', ASME/ASLE; 1981.
6. J. A. Greenwood: 'Analysis of elliptical Hertzian contacts', *Tribol. Int.*, 1997, **30**, (3), 235–237.
7. L. Houpert: 'An engineering approach to Hertzian contact elasticity: Part I', *J. Tribol.*, 2001, **123**, (3), 582–588.
8. J. -F. Antoine, C. Visa, C. Sauvey and G. Abba: 'Approximate analytical model for Hertzian elliptical contact problems', *J. Tribol.*, 2006, **128**, 660–664.
9. R. L. Jackson and I. Green: 'On the modeling of elastic contact between rough surfaces', *Tribol. Trans.*, 2011, **54**, (2), 300–314.
10. R. Malayalamurthi and R. Marappan: 'Elastic-plastic contact behavior of a sphere loaded against a rigid flat', *Mech. Adv. Mater. Struct.*, 2008, **15**, (5), 364–370.
11. L. Kogut and I. Etsion: 'A finite element based elastic-plastic model for the contact of rough surfaces', *Tribol. Trans.*, 2003, **46**, (3), 383–390.
12. L. Kogut and I. Etsion: 'A static friction model for elastic-plastic contacting rough surfaces', *J. Tribol.*, 2004, **126**, (1), 34–40.
13. R. L. Jackson and I. Green: 'A finite element study of elasto-plastic hemispherical contact against a rigid flat', *J. Tribol.*, 2005, **127**, (2), 343–354.
14. J. A. Greenwood and J. B. P. Williamson: 'Contact of nominally flat surfaces', *Proc. R. Soc. Lond. A*, 1966, **295A**, (1442), 300–319.
15. Y. Zhao, D. M. Maietta and L. Chang: 'An asperity microcontact model incorporating the transition from elastic deformation to fully plastic flow', *J. Tribol.*, 2000, **122**, (1), 86–93.
16. W. R. Chang, I. Etsion and D. B. Bogy: 'An elastic-plastic model for the contact of rough surfaces', *J. Tribol.*, 1987, **109**, (2), 257–263.
17. J. A. Greenwood and J. H. Tripp: 'The elastic contact of rough spheres', *J. Appl. Mech.*, 1967, **89**, 153.
18. J. A. Greenwood and J. J. Wu: 'Surface roughness and contact: an apology', *Meccanica*, 2001, **36**, (6), 617–630.
19. B. B. Mikic and R. T. Roca: 'A solution to the contact of two rough spherical surfaces', *J. Appl. Mech.*, 1974, **41**, 801.
20. J. A. Greenwood, K. L. Johnson and E. Matsubara: 'A surface roughness parameter in Hertz contact', *Wear*, 1984, **100**, (1–3), 47–57.
21. A. Jourani: 'A new three-dimensional numerical model of rough contact: influence of mode of surface deformation on real area of contact and pressure distribution', *J. Tribol.*, 2014, **137**, (1), 011401–011401.
22. M. Bahrami, M. M. Yovanovich and J. R. Culham: 'A compact model for spherical rough contacts', *J. Tribol.*, 2005, **127**, (4), 884–889.
23. S. U. Butt, J. -F. Antoine and P. Martin: 'An analytical model for repositioning of 6 D.O.F fixturing system', *Mech. Ind.*, 2012, **13**, (03), 205–217.
24. T. Tsukada and Y. Anno: 'On the approach between a sphere and a rough surface (1st. report – analysis of contact radius and interface pressure', *J. Jpn Soc. Precis. Eng.*, 1979, **45**, (4), 473–479.
25. J. Kagami, K. Yamada and T. Hatazawa: 'Contact between a sphere and rough plates', *Wear*, 1983, **87**, (1), 93–105.
26. M. Bahrami: 'Modeling of thermal joint resistance for sphere-flat contacts in a vacuum'; 2004, Waterloo, Ont., University of Waterloo.
27. E. Kreyszig: 'Advanced engineering mathematics'; 2007, New Delhi, Wiley-India.
28. M. Abramowitz and I. A. Stegun: 'Handbook of mathematical functions with formulas, graphs, and mathematical tables'; 1972, New York, Dover.
29. G. Nemes: 'New asymptotic expansion for the gamma function', *Arch. Math.*, 2010, **95**, 161–169.
30. J. H. Yeh and F. W. Liou: 'Contact condition modelling for machining fixture setup processes', *Int. J. Mach. Tools Manuf.*, 1999, **39**, (5), 787–803.
31. S. U. Butt: 'Design and modelling of a fixturing system for an optimal balancing of a part family', PhD thesis, Arts et Métiers ParisTech, Metz, France; 2012.